ELSEVIER

Journal of Non-Crystalline Solids 254 (1999) 17–25

JOURNAL OF NON-CRYSTALLINE SOLIDS

www.elsevier.com/locate/jnoncrysol

First principle calculations of the optical properties of a neutral oxygen vacancy in Ge-doped silica

Gianfranco Pacchioni *, Andrea Basile

Istituto Nazionale di Fisica della Materia, Dipartimento di Scienza dei Materiali, Università di Milano–Bicocca, via Cozzi 53, 20125 Milan, Italy

Abstract

We report ab initio configuration interaction calculations of the optical properties of a neutral oxygen vacancy in Ge-doped silica. This defect center, V(SiGe), is assumed to involve a missing O atom between a Si and a Ge atom with formation of a direct Si—Ge bond, ≡Si—Ge≡. Several calculations have been performed using cluster models to obtain a reliable estimate of the excitation energy. The lowest fully allowed singlet–singlet transition in V(SiGe) occurs in a spectral region around 7.3 eV according to the calculations, i.e. not too far from the absorption band at 7.6 eV attributed to a V(SiSi) center in pure silica. The emission properties of V(SiGe) and the reasons for the similar transition energy in V(SiSi) and V(SiGe) centers are discussed.

PACS: 31.25.Qm; 42.70.Ce; 61.72.Ji; 61.72.Bb; 78.20.-e

1. Introduction

Germanium dioxide is widely used in the fabrication of optical fibers to increase the refractive index of glassy silica [1]. The presence of Ge in the fiber results in a larger dependence of the optical properties of the material on external factors and fabrication conditions. This dependence has been generally attributed to the presence of germanium-related defects. For this reason several studies have been devoted to the optical properties of point defects, and in particular of defects usually denoted as oxygen deficient centers (ODC), in pure GeO_2 and in Ge-doped SiO_2 [1–9]. Recently, vacancies in Ge-doped silica glasses have been related to increased effects of second harmonic generation and photoinduced refractive index gratings in optical fibers [10–12]. The study of these centers is complicated by at least two facts: (a) the native variants of ODC are diamagnetic and are therefore undetectable by electron paramagnetic resonance experiments; (b) both intrinsic and extrinsic ODC are present in SiO_2:Ge based materials. For these reasons, a detailed description of the structural defects responsible for the optical properties of Ge-doped silica has not been possible so far. ODCs have been proposed as the origin of a series of UV absorption bands in SiO_2:Ge located around 5.2 and 6.7–7.3 eV [1,2,13] accompanied by two prominent photoluminescence bands at ≈4.3 and 3.2 eV [1] (usually referred to as the α and β bands). It should be mentioned that the nature and origin of the 168 nm band in Ge-doped silica (7.3 eV) is still controversial [1,13]. In fact, the bands near this wavelength have complicated properties

* Corresponding author. Tel.: +39-02 6617 4219; fax: +39-02 6617 4403; e-mail: gianfranco.pacchioni@mater.unimib.it

0022-3093/99/$ – see front matter
PII: S0022-3093(99)00369-5

probably due to the existence of different variants of the same defect [13]. These features are quite similar to those observed in pure silica where absorption bands at 5.0 eV (B_2 band) and at 7.6 eV (E band) give rise to typical photoluminescence bands at 4.4 and 2.7 eV. Several tentative assignments have been proposed for the 5.0 and 7.6 optical absorption bands in pure silica [14–19].

In a recent series of papers we have reported ab initio calculations on the photoabsorption and photoluminescence properties of ODCs in silica [20,21] including the neutral oxygen vacancy, V(SiSi). Here we briefly review the results. We found that the V(SiSi) center exists in two configurations, one of which is metastable. A $S_0 \rightarrow S_1$ (singlet–singlet) transition occurs at 7.5 eV [20]. The transition is followed by a vibrational relaxation to the minimum of the excited state. The radiative decay, $S_1 \rightarrow S_0$, from this minimum is computed at 4.3 eV; this mechanism has been proposed as the origin of the photoluminescence observed experimentally in this region. We also tentatively suggested that the 5.0 eV absorption band (B_2) is due to the vertical transition from a metastable form of the V(SiSi) center, a 'puckered' structure which can be schematically represented as $\equiv Si^{+} - {}^{-} Si \equiv$, to the S_2 excited state [20]. Through a different vibrational channel, the system relaxes to the same minimum of the S_1 excited state reached by the 7.6 eV absorption. The model accounts for the fact that the same photoluminescence at 4.4 eV is stimulated by excitation in both E and B_2 regions and is consistent with the correlation between the bleaching of the B_2 band and the increase of the concentration of the E' centers (an oxygen vacancy with a trapped hole). On the other hand, it implies a considerable population of a metastable state to account for the intensity of the B_2 band, a fact which is unlikely given the high energy, $\approx$2.7 eV, separating the metastable state from the global minimum. A completely different model to explain the B_2 absorption band (5.0 eV) and the corresponding emissions at 4.4 and 2.7 eV has been proposed years ago by Skuja [22]. The model is based on a two-coordinated Si, a Si atom bonded to two oxygen atoms, =Si:. In a recent work we have investigated the optical properties of this center and of the Ge-related analogs, =Ge: [23]. The lowest transition, $S_0 \rightarrow T_1$, (very weak because forbidden by the spin selection rules) for =Si: is found at 3.0 eV, in excellent agreement with the experiment, 3.2 eV [22]. The $S_0 \rightarrow T_1$ absorption for =Ge: is computed at $\approx$3.2 eV (3.7 eV in the experiment [22]). The first allowed vertical transition, $S_0 \rightarrow S_1$, is computed 5.2 eV for =Si: and at 5.4 eV for =Ge: [23]. Both energies are consistent with the position of the B_2 band in SiO_2 and SiO_2:Ge. The experimental $T_1 \rightarrow S_0$ emission, computed at 2.6 eV [23], occurs experimentally at 2.7 eV with a decay time of 10 ms in SiO_2 [22]. Also for the =Ge: center the computed $T_1 \rightarrow S_0$ emission, 2.8 eV [23], is reasonably close to the measured one, $\approx$3.1 eV.

The second, and more important, emission considered is the photoluminescence band at 4.4 eV. For pure silica we computed a $S_1 \rightarrow S_0$ emission at 4.6 eV with a lifetime $\tau = 5.5$ ns, in excellent agreement with the experiment [22]. For =Ge: the agreement between theory and experiment for the $S_1 \rightarrow S_0$ decay is less satisfactory since the experimental energy is 4.3 eV [22] while our computed energy is 5.0 eV [23]. The Stoke shift, which in the experiment is of 0.8 eV, is 0.4 eV only in the calculations probably because correlation effects have not been included in the geometrical optimization of the excited state. To summarize, the observed optical transitions and radiative lifetimes have been quantitatively or almost quantitatively reproduced for Si and for the isovalent Ge two-coordinated center [23]. Similar results have been obtained independently by Stefanov and Ragavachari [9]. Furthermore, the magnetic interactions in the corresponding hydrogenated centers are also correctly reproduced by the calculations [23]. Thus, the results support the idea that two-coordinated Si and Ge centers are responsible for the optical activity stimulated by 5.0–5.2 eV photons.

In this work we report new results on the optical properties of a neutral oxygen vacancy in SiO_2:Ge, V(SiGe). We have performed calculations of the optical absorptions and emission properties of a V(SiGe) center and we have compared the results with new calculations performed at the same level on the V(SiSi) defect. The results

provide new important insight into the dynamics of oxygen deficient centers in pure and Ge-doped silica.

2. Computational approach

An oxygen vacancy in Ge-doped silica has been modeled by $(OH)_3Si{-}Ge(OH)_3$, Fig. 1, and $Si_{13}GeO_{16}H_{26}$, Fig. 2, clusters. In both cases the cluster dangling bonds have been saturated by H atoms, a commonly used technique to 'embed' clusters of semiconducting or insulating materials [8,9,20,21,23]. The positions of the cluster atoms were initially fixed to those of α-quartz. The embedding H atoms were fixed at a distance of 1.48 and 0.98 Å, respectively, from the Si and O atoms along the Si—O directions of α-quartz. The position of all the Si and O atoms of the cluster has been fully optimized. The fixed H atoms provide a simple representation of the mechanical embedding of the solid matrix. For comparison, calculations have also been performed relaxing the positions of the H atoms. This second approach models a more flexible network than α-quartz, similar to that of amorphous silica.

The cluster wave functions have been constructed using local Gaussian type atomic orbitals basis sets. The Si and Ge atoms have been represented either with all their electrons, AE, or by

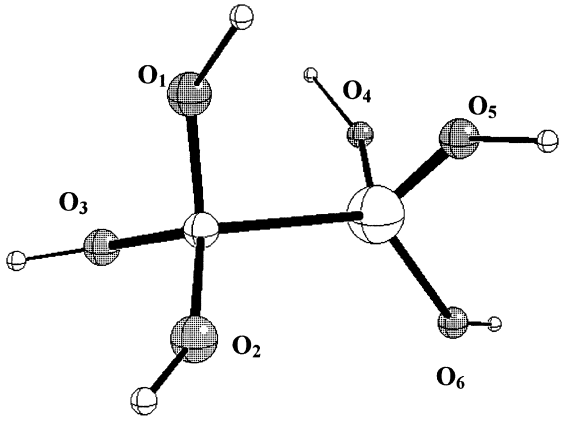

Fig. 1. $(HO)_3Si{-}Ge(OH)_3$ model of a neutral oxygen vacancy in Ge-doped silica. White spheres: Si or Ge; large gray spheres, O; small white spheres: H.

Effective Core Potentials (ECP) which include explicitly in the valence only the ns^2np^2 electrons [24,25]. For Ge a relativistic ECP has been used [25]. We used a (4s4p/2s2p) ECP basis set [24,25] on Si and Ge augmented by a d polarization function ($\alpha_d(Si) = 0.395$, $\alpha_d(Ge) = 0.15$) and one set of diffuse s and p functions ($\alpha_{Si} = 0.035$, $\alpha_{Ge} = 0.040$). AE MIDI-4 [26] and MINI-1 [27] basis sets were used on the O and on the terminating H atoms, respectively. The validity of the ECP has been tested by comparing the results with those of AE calculations with basis sets of comparable size; in particular, we used a 6-31G* basis set on Si [28], a 3-21G* [29] and an even tempered (ET) (17s13p8d/6s5p2d) [30] AE basis sets on Ge. These basis sets contain or have been augmented by diffuse s and p and one d polarization functions with similar exponents to those used with the ECP basis sets. The differences in the geometry due to the basis set or ECP used are negligible, while the computed excitation energies differ at most by 0.1 eV. Geometry optimizations have been performed at the restricted (open) Hartree–Fock levels, RHF or ROHF, for closed shell singlet and open shell triplet states, respectively, and at the generalized valence bond, GVB, level for open shell singlets states by computing analytical gradients of the total energy. Given the local symmetry of the defect, all the clusters are computed without any symmetry element (C_1 symmetry group).

Correlation effects have been included by performing multi-reference single- and double-excitations configuration interaction calculations, MRD CI, for the ground and the excited states of the clusters [31,32]. Single and double excitations with respect to more than one reference or main configuration (M) are generated; in this way it is possible to include directly higher excitation classes with respect to the leading configuration in the final CI results. The method makes use of an extrapolation technique; only those configurations with an estimated contribution to the total CI energy larger than a given threshold, T, are included in the secular determinant; the contribution to the final CI energy of the remaining configurations is estimated perturbatively based on an extrapolation technique. Twenty-six valence electrons have been correlated for each

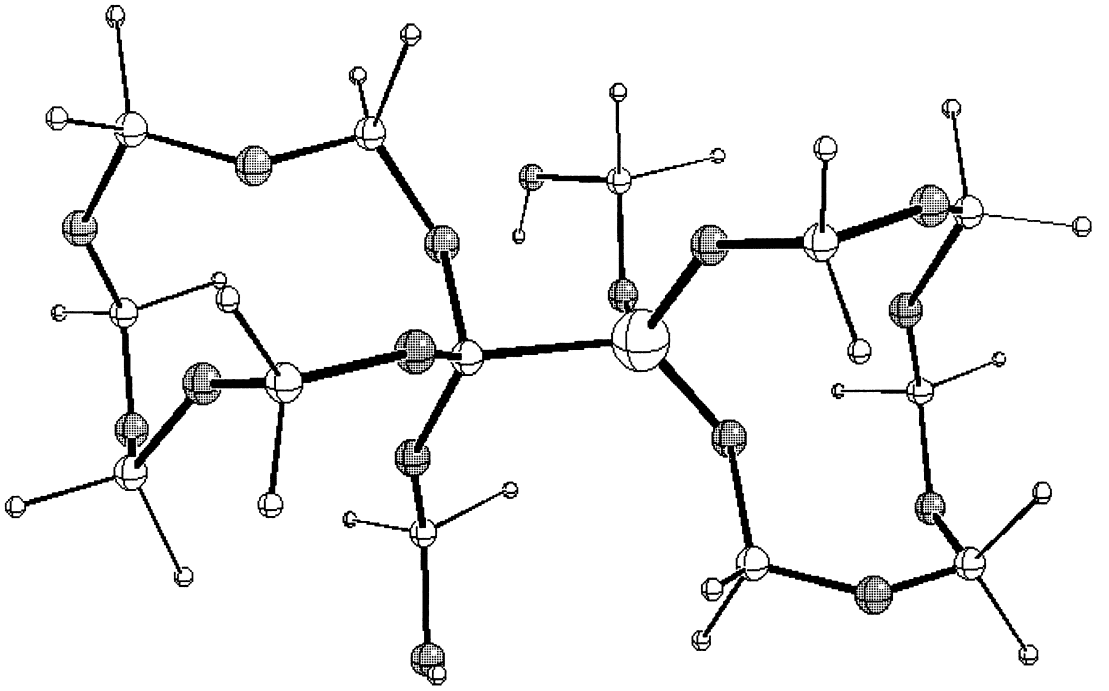

Fig. 2. $Si_{13}GeO_{16}H_{26}$ model of a neutral oxygen vacancy in Ge-doped silica. White spheres: Si or Ge; large gray spheres, O; small white spheres: H.

Si—or Ge-containing cluster. Typically, a few thousand configurations are directly included in the secular problem, while the number of generated configurations can be 1–10 millions. The reported CI energies are extrapolated to this larger CI space. All configurations contributing more than 0.1% to the final CI wave function are used as main (M) configurations. Specific details of the CI calculations are given in Table 3. Singlet-to-singlet, $S_0 \rightarrow S_1$, and singlet-to-triplet, $S_0 \rightarrow T_1$, transitions and the corresponding emissions have been considered.

Absorption intensities have been estimated by means of the oscillator strength, f, computed using the dipole-length operator as

$$f(\mathbf{r}) = 2/3| < \psi_{e''}|e\mathbf{r}|\psi_{e'} > |^2 \Delta E, \quad (1)$$

where ΔE is the calculated transition energy. The value of f for a fully allowed transition is of the order of 0.1 to 1. From the $f(r)$ also the expected lifetimes of the excited states, τ, have been determined.

The calculations have been performed using the HONDO-8 [33], Gaussian94 [34] and Gamess-UK [35] program packages.

3. Neutral oxygen vacancy in Ge-doped silica

The substitution of a four-coordinated Si atom by Ge in Ge-doped silica has an important consequence from the thermodynamic point of view. In fact, the Ge—O bond is weaker than the Si—O one and the formation energy of an oxygen vacancy at a ≡Si—O—Ge≡ site is predicted to be less than at a ≡Si—O—Si≡ site by about 1 eV [36]. The consequence is that a large number of defects, in particular vacancies, are expected to form in correspondence to the Ge atoms. The simplest model of an oxygen vacancy in SiO_2:Ge is therefore a center where an oxygen is missing between a Si and a Ge nearest neighbors, ≡Si—Ge≡ or V(SiGe). Starting from the assumption that these centers are present in Ge-doped silica, the

following question is to which extent the optical absorption and emission properties of a V(SiGe) center resemble those of a corresponding V(SiSi) center. The problem has been addressed in a recent theoretical paper by Stefanov and Ragavachari [9] who performed ab initio calculations on the lowest vertical transition of V(SiGe) and V(SiSi). Correlation effects, essential for the proper description of the excited state, have been introduced at the CIS(D) level, a configuration interaction approach with single substitutions and second-order perturbative correction for double substitutions [9]. The results give similar absorption energies for V(SiSi) and V(SiGe), with absorption bands centered around 6.7–7.0 eV [9]. For V(SiSi), these energies are about 0.6 eV less than the intense band observed at 7.6 eV in the experiment [14,16,17] and of 7.5 eV computed by our approach [20]. Here we consider the same excitation within a slightly different computational scheme and we extend the analysis of the optical properties of this center to other states (triplet) and to the emission features.

Before discussing the optical properties, we consider the geometry of a V(SiGe) center. Two variants of the $(HO)_3Si{-}Ge(OH)_3$ minimum cluster model, Fig. 1, have been considered, one with the terminal H atoms fixed in space during the optimization so that the internal torsions of the cluster simulate those of α-quartz (H-fixed model), and one where the H atoms have been let completely free to relax (H-free model). This latter model can be considered as a more appropriate representation of the structure of amorphous silica. A larger model, $Si_{13}GeO_{16}H_{26}$, Fig. 2, includes two complete Si—O rings. The position of the H atoms at the cluster periphery has been fixed but the larger size of the cluster gives a greater flexibility to the Si—O network to respond to the oxygen removal. The results of the geometry optimizations performed at the Hartree–Fock level are shown in Table 1. The formation of a V(SiGe) center results in a short Si—Ge distance. The small H-fixed model gives a Si—Ge bond distance of 2.48 Å, practically identical to that computed for a V(SiSi) center using a similar cluster, $(HO)_3Si{-}Si(OH)_3$, and basis set, Table 2. It is interesting to note that the distance in V(SiGe) and V(SiSi) is similar despite the larger size of the Ge atom. On the other hand, the Ge—O bond lengths are considerably longer than the Si—O ones, see Tables 1 and 2, resulting in a similar distance of the two group IV atoms in V(SiGe) and V(SiSi).

The H-free model and the larger cluster, allowing a larger relaxation, give Si—Ge distances which are about 0.1 Å shorter than in the H-fixed model, Table 1. With the H-free model the computed r(Si—Ge) ≈ 2.38 Å is practically the same

Table 1
Bond distances (Å), for ground, S_0, and excited states, T_1 and S_1, of an oxygen vacancy in Ge-doped silica, V(SiGe), Fig. 1

Cluster	Structure and state	Si—Ge	Si—O_1	Si—O_2	Si—O_3	Ge—O_4	Ge—O_5	Ge—O_6
$SiGeO_6H_6$, H-fixed	≡Si—Ge≡, S_0	2.490	1.625	1.632	1.628	1.779	1.782	1.779
$SiGeO_6H_6$, H-free	≡Si—Ge≡, S_0	2.362	1.608	1.624	1.615	1.754	1.771	1.769
$Si_{13}GeO_{16}H_{26}$	≡Si—Ge≡, S_0	2.379	1.609	1.603	1.610	1.708	1.721	1.701
$SiGeO_6H_6$, H-fixed	≡Si• •Ge≡, T_1	3.546	1.642	1.630	1.633	1.758	1.760	1.765
$SiGeO_6H_6$, H-fixed	≡Si• •Ge≡, S_1	3.640	1.642	1.631	1.635	1.758	1.758	1.763

Table 2
Bond distances (Å), for ground, S_0, and excited states, T_1 and S_1, of an oxygen vacancy in pure silica, V(SiSi), Fig. 1

Cluster	Structure and state	Si—Ge	Si—O_1	Si—O_2	Si—O_3	Si—O_4	Si—O_5	Si—O_6
$Si_2O_6H_6$, H-fixed	≡Si—Si≡, S_0	2.478	1.655	1.639	1.648	1.654	1.652	1.647
$Si_2O_6H_6$, H-free	≡Si—Si≡, S_0	2.300	1.622	1.633	1.628	1.623	1.638	1.626
$Si_2O_6H_6$, H-fixed	≡Si• •Si≡, T_1	3.694	1.631	1.628	1.630	1.644	1.632	1.635
$Si_2O_6H_6$, H-fixed	≡Si• •Si≡, S_1	3.759	1.630	1.628	1.630	1.643	1.633	1.635

obtained by Stefanov and Ragavachari [9]. Therefore, the estimated distance in V(SiGe) is $\approx 2.43 \pm 0.05$ Å. In principle, the Si—Ge distance can have important consequences on the optical transitions. For this reason, we have considered both H-free and H-fixed models for the computation of the lowest $S_0 \rightarrow S_1$ transition in V(SiGe). We also checked the stability of the CI results by comparing various basis sets and CI expansion, Table 3. In all cases diffuse functions have been included in the Si and Ge basis sets to account for the Rydberg states of the system. In fact, previous work on V(SiSi) as well as on the Si_2H_6 molecule [20] has shown the Rydberg character of the high excited states associated with the Si—Si bond. We used the same geometry of the $(HO)_3Si—Ge(OH)_3$ cluster (H-fixed or H-free) for all CI calculations. In this way we have been able to analyze the dependence of the results on the level of CI treatment. Of course, since the calculations are not performed from a minimum structure, the transition energies are in error by a few tenths of an eV. More refined CI calculations performed from the optimal structure will be discussed below, see Tables 4 and 5.

From the combination of the sp^3 hybrid orbitals on the Si and Ge atoms of the defect, a doubly occupied σ bonding and an empty σ^* antibonding state appear in the band gap. The ground state, S_0, is therefore $(\sigma)^2(\sigma^*)^0$. The first allowed transition is S_0 $(\sigma)^2(\sigma^*)^0 \rightarrow S_1$ $(\sigma)^1(\sigma^*)^1$ with formation of two singly occupied dangling bonds, coupled singlet, on the adjacent Si and Ge atoms, ≡Si• •Ge≡. In a first set of CI calculations we used the H-fixed model and an AE basis set on both Si and Ge atoms (the O atoms are always treated with a AE MIDI-4 basis). For Si and Ge we used a 6-31G*(sp) and a 3-21G*(sp) AE basis

Table 3
Computed $S_0 \rightarrow S_1$ transition energies and intensities of a neutral oxygen vacancy, V(SiGe), as function of the details of the calculation[a]

Si basis set	Ge basis set	T[c]	Active space[d]	H-fixed[b]			H-free[(b)]		
				nM/nR[e]	T_e (eV)	f[f]	nM/nR[e]	T_e (eV)	f[f]
AE 6-31G*(sp)	AE 3-21G*(sp)	10	49 (116)	21M/2R	7.62	0.41	24M/2R	7.71	0.14
AE 6-31G*(sp)	AE ET (6s5p2d)(sp)	10	49 (116)	28M/2R	7.59	0.25	28M/2R	8.08	0.12
ECP (2s2p1d)(sp)	ECP (2s2p1d)(sp)	10	56 (96)	12M/2R	7.75	0.45	28M/2R	7.92	0.09
ECP (2s2p1d)(sp)	ECP (2s2p1d)(sp)	5	56 (96)	11M/2R	7.71	0.47	26M/2R	8.03	0.08

[a] The calculations have been performed for a fixed geometry obtained using the following basis sets: Si AE 6-31G*, Ge ECP (2s2p1d), O 6-31G, H MINI-1.
[c] Threshold for configuration selection (see text).
[d] Total number of active occupied and virtual orbitals; 26 electrons have been correlated. In parenthesis the total number of orbitals is given.
[b] Cluster model with free or fixed terminal H atoms in the geometry optimization (see text).
[e] Number of Main configurations, M, and of Roots, R.
[f] Oscillator strength.

Table 4
Optical properties of an oxygen vacancy, V(SiGe), in Ge-doped silica[a]

Transition	nM/nR[b]	T[c] (μhartree)	T_e (eV)	f[d]	τ[e] (s)	Exp.
$S_0 \rightarrow S_1$	11M/2R	10	7.33	0.45	1×10^{-9}	6.7–7.3 [1,2]
$S_1 \rightarrow S_0$	10M/2R	10	4.02	0.50	3×10^{-9}	≈4.3 [22]
$S_0 \rightarrow T_1$	11M/2R (S_0) 1M/1R (T_1)	10	7.00	Forbidden	–	Not observed
$T_1 \rightarrow S_0$	1M/1R (T_1) 6M/1R (S_0)	10	0.83	Forbidden	–	≈3.2 [22]

[a] The calculations refer to a $(HO)_3SiGe(OH)_3$ cluster using a (2s2p1d)(sp) ECP basis set on Si and Ge and a MIDI-4 and MINI-1 AE basis sets on O and H, respectively. 26 electrons have been correlated.
[b] Number of Main configurations, M, and of Roots, R.
[c] Threshold for configuration selection (see text).
[d] Oscillator strength.
[e] Lifetime.

Table 5
Optical properties of an oxygen vacancy, V(SiSi), in silica[a]

Transition	nM/nR[b]	T[c] (μhartree)	T_e (eV)	f[d]	τ[e] (s)	Exp.
$S_0 \rightarrow S_1$	9M/2R	10	7.94	0.44	8×10^{-10}	≈7.6 [14]
$S_1 \rightarrow S_0$	10M/2R	10	4.65	0.56	2×10^{-9}	≈4.4 [22]
$S_0 \rightarrow T_1$	9M/2R (S_0) 1M/1R (T_1)	10	6.90	Forbidden	–	Not observed
$T_1 \rightarrow S_0$	1M/1R (T_1) 4M/1R (S_0)	10	0.57	Forbidden	–	≈2.7 [22]

[a] The calculations refer to a $(HO)_3SiSi(OH)_3$ cluster using a (2s2p1d)(sp) ECP basis set on Si and a MIDI-4 and MINI-1 AE basis sets on O and H, respectively. 26 electrons have been correlated.
[b] Number of Main configurations, M, and of Roots, R.
[c] Threshold for configuration selection (see text).
[d] Oscillator strength.
[e] Lifetime.

set [28,29], respectively, where (sp) indicates the addition of one diffuse s and one diffuse p functions. The $S_0 \rightarrow S_1$ T_e obtained with this basis is 7.62 eV. Using a more flexible ET AE basis set for Ge [30], the T_e, 7.59 eV, is practically identical, Table 3. We repeated the calculations using an ECP on both Si and Ge atoms [24,25]. The use of an ECP has two advantages: it reduces the size of the basis set thus allowing inclusion of more virtual orbitals in the active space and, for Ge, takes into account scalar relativistic effects. The results, however, do not change significantly: the computed T_e is 7.7 eV. When the calculations are performed using the geometry of the H-free model (shorter Si—Ge distance, Table 2), the $S_0 \rightarrow S_1$ T_es become ≈0.3 eV larger, ≈8 eV, Table 3. Therefore, we found that (a) the use of an ECP on Si or Ge does not affect the quality of the results and (b) the effect of the geometry on the $S_0 \rightarrow S_1$ transition is not larger than 0.3 eV. The data of Table 3 show a substantial stability of the results versus the details of the calculations.

To obtain a more accurate estimate of the absorption and emission properties we performed a new set of CI calculations. Using an ECP on both Si and Ge atoms, Table 4, but starting from a fully optimized geometry, Table 2, the $S_0 \rightarrow S_1$ vertical transition in V(SiGe) occurs at 7.3 eV; this energy is in excellent agreement with the observed band at 168 nm (7.3 eV) [1,2,13]. It should be noted however that all the computed transitions have error bars of at least ±0.3 eV. It is also interesting to note that the oscillator strength is ~1, Table 4. In this respect a considerable difference is found between the results obtained with the H-fixed and H-free models, see Table 3. The oscillator strength is proportional to the matrix element between the ground and excited state wave functions; the fact that the oscillator strength is about 5 times larger for the H-fixed model, where the Si—Ge distance is longer, indicates that the overlap with the excited state wave function is larger. This difference brings us directly into the problem of the structural relaxation of the excited state.

The rupture of the Si—Ge bond due to the absorption of a high-energy photon causes a substantial geometrical relaxation of the S_1 excited state. The geometry optimization of the excited state has been performed with the H-fixed model. In fact, the rupture of the Si—Ge bond would result in a complete dissociation of the $Si(OH)_3$ and $Ge(OH)_3$ fragments in absence of a mechanical constraint. Using a GVB wave function for the open shell singlet S_1 state and analytical gradients we found that in the minimum configuration the Si and Ge atoms move ≈3.65 Å apart. From the minimum of the S_1 excited state the system decays to S_0. The computed energy of the emitted photon is of 4.0 eV with a Stokes shift of 3.3 eV. The lifetime of the emission process, 3 ns, is very short. Thus, a neutral oxygen vacancy V(SiGe) can in principle give rise to an emission around 4 eV due to a radiative $(\sigma)^1(\sigma^*)^1 \rightarrow (\sigma)^2$ decay from the minimum of the S_1 $\equiv Si^{\bullet}\ ^{\bullet}Ge\equiv$ excited state. This could be tentatively associated with the 4.3 eV emission observed in Ge-doped silica [22]. However, it should be noted that a similar emission occurs in correspondence of two-coordinated Ge centers [22,23]. We consider now the $S_0 \rightarrow T_1$ transition and the corresponding $T_1 \rightarrow S_0$ emis-

sion. The vertical $S_0 \rightarrow T_1$ excitation occurs at 7.0 eV, Table 4. Singlet–triplet transitions, $S_0 \rightarrow T_1$, however, are spin forbidden and can carry sufficient intensity only through spin–orbit coupling. Unfortunately, this makes a detection of the singlet–triplet excitations very difficult in general and prohibitive in this case where the absorption band is completely covered by the intense $S_0 \rightarrow S_1$ absorption. A large geometrical relaxation occurs also for the triplet state, T_1 $(\sigma)^1(\sigma^*)^1$ (ROHF wave function), although slightly smaller than for the S_1 state; the Si—Ge distance increases to 3.5 Å. The emission from the minimum of the excited triplet state takes place in our calculations at 0.83 eV, Table 4. This is very far from the typical luminescence at 3.2 eV observed for SiO_2:Ge samples.

The optical properties of the V(SiGe) center have been compared to those of the isovalent V(SiSi) center. We have repeated the calculations for the singlet–singlet and singlet–triplet transitions using exactly the same cluster and basis set size used for V(SiGe), Table 5. The $S_0 \rightarrow S_1$ transition occurs at 7.9 eV (7.5 eV is our previously reported energy [20]); it is reasonably close to the experimental band at 7.6 eV in pure silica [14]. This agreement confirms our previous assignment of the 7.6 eV E band to a neutral oxygen vacancy [20]. The $S_0 \rightarrow S_1$ absorption occurs therefore at a larger energy, about 0.6 eV, in V(SiSi) than in V(SiGe). The $S_1 \rightarrow S_0$ decay occurs at 4.65 eV and, again, is about 0.6 eV larger than for the analogous center with Ge; our previous estimate for this emission was 4.3 eV [20]. The energy and lifetime of the emission are not inconsistent with the observed luminescence at 4.4 eV [22]. The $S_0 \rightarrow T_1$ excitation requires 6.9 eV in V(SiSi), and is similar to what found for V(SiGe), see Tables 4 and 5. The inverse process, $T_1 \rightarrow S_0$, corresponds to an emission at 0.57 eV, even smaller than that computed for the Ge-containing center, 0.83 eV. Both energies are too small to account for the observed triplet–singlet emission bands observed at 2.7 and 3.2 eV in pure and Ge-doped silica, respectively [22]. This result casts serious doubts on the decay mechanism from the excited triplet (and singlet) states of V(SiGe) as a possible origin of the 4.3 and 3.1 eV bands observed experimentally in Ge-doped silica, as it will be discussed in the next section.

4. Discussion and conclusions

The neutral oxygen vacancy in pure or Ge-doped silica, V(SiSi) or V(SiGe), consists of a direct Si—Si or Si—Ge bond of similar length, about 2.4 Å; from the ground state of the defect, the first fully allowed vertical transition is computed at 7.9 eV, V(SiSi), and at 7.3 eV, V(SiGe). Both energies are quite close to the observed intense bands at 7.6 eV in SiO_2 [14] and 6.7–7.3 eV in SiO_2:Ge [1,2,13]. Thus, we assume that the origin of these bands should be attributed to the neutral oxygen vacancy. In the case of Ge-doped silica, however, this assignment is less certain due to the complex properties of the 168 nm band [13]. The quite similar transition energy in V(SiSi) and V(SiGe) is largely due to the similar geometric and electronic structures of the defect. In both cases, in fact, a filled bonding and an empty antibonding σ state appear in the gap of the material; the $\sigma \rightarrow \sigma^*$ transition is responsible for the optical absorption in both defects. Also the singlet–triplet excitation occurs at similar energies, about 7.0 eV, in V(SiSi) and V(SiGe).

The decay from the S_1 excited state to the S_0 ground state is accompanied by the emission of a 4.6 eV photon in V(SiSi) and of 4.0 eV photon in V(SiGe). These two features are relatively close to the observed emissions at 4.4 and 4.3 eV in pure and Ge-doped [22] silica, respectively; these bands can be attributed to the decay from the excited state of a neutral oxygen vacancy. However, the 4.4 and 4.3 eV experimental bands are always accompanied by typical emissions at 2.7 and 3.2 eV due to a triplet-to-singlet decay [22]. In our calculations this decay corresponds to an emitted photon of 0.6 eV in V(SiSi) and 0.8 eV in V(SiGe). These energies are too far from the experimental energies to support the assignment of the experimental bands at 2.7 and 3.2 eV to the $T_1 \rightarrow S_0$ emission of a neutral oxygen vacancy. Thus, the decay mechanism is probably more complex or involves a different center. In this respect, our previous study [23] on the two-coordinated Si and Ge centers, =Si: and =Ge:, shows that the computed optical properties of these defects fully account for the observed absorption at 5.0 eV (SiO_2) and 5.2 eV (SiO_2:Ge) and for the corresponding

4.4 and 2.7 eV (SiO_2) or 4.3 and 3.2 eV (SiO_2:Ge) emissions, as suggested by Skuja [18,22]. What remains unknown is why the absorption of a high-energy photon (7.3–7.6 eV), due to the V(SiSi) or V(SiGe) centers, can give rise to the typical emission features of a two-coordinated defect. In this respect it is worth mentioning the recently discussed mechanism [37] of internal conversion of a neutral oxygen vacancy into a di-coordinated center upon excitation in vacuum-UV according to the reaction:

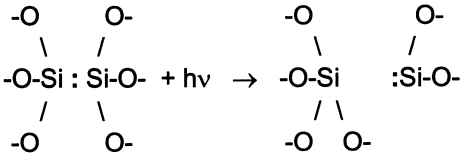

In this process a neutral oxygen vacancy, ≡Si—Si≡ is converted upon excitation into a di-coordinated, =Si:, and a four-coordinated, =Si=, centers. The process, however, is likely to require relatively high energies. The mechanism of conversion is unknown. More work is required to verify this hypothesis.

Acknowledgements

We thank Dr Linards Skuja for the critical reading of the manuscript and for the useful discussions. This work has been partially supported by the Air Force Office of Scientific Research, European Office of Aerospace Research and Development through contract # F61775-98-WE067.

References

[1] V.B. Neustruev, J. Phys:. Condens. Matter 6 (1994) 6901.
[2] M.J. Yuen, Appl. Opt. 21 (1982) 136.
[3] M.K. Schurman, M. Tomozawa, J. Non-Cryst. Solids 202 (1996) 93.
[4] K. Awazu, H. Onuki, K. Muta, J. Non-Cryst. Solids 211 (1997) 158.
[5] B. Crivelli, M. Martini, F. Meinardi, A. Paleari, G. Spinolo, Phys. Rev. B 54 (1996) 16637.
[6] M. Martini, F. Meinardi, A. Paleari, G. Spinolo, A. Vedda, Phys. Rev. B 57 (1998) 3718.
[7] F. Meinardi, A. Paleari, Phys. Rev. B 58 (1998) 3511.
[8] V.B. Sulimov, V.O. Sokolov, B. Poumellec, Phys. Stat. Sol. B 196 (1996) 175.
[9] B.B. Stefanov, K. Ragavachari, Phys. Rev. B 56 (1997) 5035.
[10] T.E. Tsai, M.A. Saifi, E.J. Friebele, D.L. Griscom, U. Osterberg, Opt. Lett. 14 (1989) 1023.
[11] K.D. Simmons, S. LaRachelle, V. Mizrahi, G.I. Stezeman, D.L. Griscom, Opt. Lett. 16 (1991) 141.
[12] H. Hosono, H. Kawazoe, K. Muta, Appl. Phys. Lett. 63 (1993) 479.
[13] B. Poumellec, H. Cens, A. Trukhin, J.C. Krupa, B. Leconte, and M. Bubnov, in: Proceedings of 12th International Conference on Optical Fiber Sensors Glass and Optical Material Division Meeting, Optical Society of America, Washington DC, 1997.
[14] H. Hosono, Y. Abe, H. Imagawa, H. Imai, K. Arai, Phys. Rev. B 44 (1991) 12043.
[15] R. Thomon, H. Mizuno, Y. Ohki, K. Sasagane, K. Nagasawa, Y. Hama, Phys. Rev. B 39 (1989) 1337.
[16] H. Imai, K. Arai, H. Imagawa, H. Hosono, Y. Abe, Phys. Rev. B 38 (1988) 12772.
[17] H. Nishikawa, R. Thomon, Y. Ohki, K. Nagasawa, Y. Hama, J. Appl. Phys. 65 (1989) 4672.
[18] L.N. Skuja, A.N. Streletsky, A.B. Pakovich, Solid State Commun. 50 (1984) 1069.
[19] R. Boscaino, M. Cannas, F.M. Gelardi, M. Leone, Phys. Rev. B 54 (1996) 6194.
[20] G. Pacchioni, G. Ieranò, Phys. Rev. Lett. 79 (1997) 753.
[21] G. Pacchioni, G. Ieranò, Phys. Rev. B 57 (1998) 818.
[22] L. Skuja, J. Non-Cryst. Solids 149 (1992) 77.
[23] G. Pacchioni, R. Ferrario, Phys. Rev. B 58 (1998) 6090.
[24] P.J. Hay, W.R. Wadt, J. Chem. Phys. 82 (1985) 270.
[25] P.J. Hay, W.R. Wadt, J. Chem. Phys. 82 (1985) 299.
[26] H. Tatewaki, S. Huzinaga, J. Comput. Chem. 1 (1980) 205.
[27] H. Tatewaki, S. Huzinaga, J. Chem. Phys. 71 (1979) 4339.
[28] R. Dichtfield, W.J. Hehre, J.A. Pople, J. Chem. Phys. 54 (1971) 724.
[29] J.S. Binkley, J.A. Pople, W.J. Hehre, J. Am. Chem. Soc. 102 (1980) 939.
[30] E. Clementi, G. Corongiu, Chem. Phys. Lett. 90 (1982) 359.
[31] R.J. Buenker, S.D. Peyerimhoff, Theoret. Chim. Acta 35 (1974) 33.
[32] R.J. Buenker, S.D. Peyerimhoff, W. Butscher, Molec. Phys. 35 (1978) 771.
[33] M. Dupuis, F. Johnston, A. Marquez, HONDO 8.5 for CHEMStation, IBM, Kingston, 1994.
[34] M.J. Frisch et al., Gaussian 94, Gaussian Inc., Pittsburgh, PA, 1997.
[35] M.F. Guest, P. Sherwood, GAMESS-UK reference manual, SERC Daresbury Laboratory, Daresbury, 1992.
[36] G. Pacchioni, G. Ieranò, Phys. Rev. B 56 (1997) 7304.
[37] L. Skuja, J. Non-Cryst. Solids 239 (1998) 16.